International Journal of Statistics and Applied Mathematics 2018; 3(3): 61-69

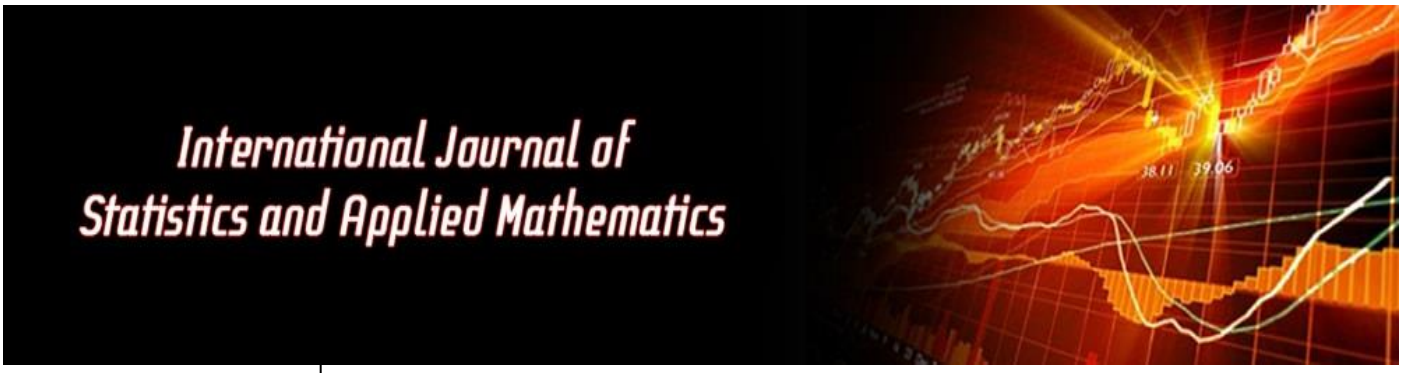

ISSN: 2456-1452
Maths 2018; 3(3): 61-69

www.mathsjournal.com
Received: 09-03-2018
Accepted: 10-04-2018

Hoshiyar Singh
Department of Mathematics,
Jaipur National University
Jaipur, Rajasthan, India

Ali Aji
Department of Mathematics,
Jaipur National University
Jaipur, Rajasthan, India

Chunni Lal
Department of Mathematics,
Jaipur National University
Jaipur, Rajasthan, India

Correspondence
Ali Aji
Department of Mathematics,
Jaipur National University
Jaipur, Rajasthan, India

Three dimensional MHD natural convection nanofluids flow with heat and mass flux from vertical surface in porous medium

Hoshiyar Singh, Ali Aji and Chunni Lal

Abstract
In This paper we investigate the MHD natural convective boundary layer flow of electrically-conducting nanofluids from a stationary vertical porous surface in a permable porous medium. The mathematical model is formulated by considering water-based nanofluids containing metallic Nano-particles for stationary plate cases. Three nanofluids are examined, namely copper, aluminum oxide or titanium oxide in water. Validation of finite element solutions for skin friction and Nusselt number is achieved via comparison with the previously published work, Primary and secondary velocities are consistently elevated with increasing Soret, thermal Grashof and solutal Grashof numbers. Increasing Schmidt number, chemical reaction and suction parameter both suppress Nano-particle concentration whereas the converse behavior is computed with increasing Soret number.

Keywords: MHD nanofluid, magnetic field, radiation, porous medium and free convection

1. Introduction
Magnetic nanofluids are growing as a new branch of possible working fluids with potential, for example, electrical transformer technologies, medical engineering and fusion power systems. These fluids are manufactured by dispersing magnetic nanoparticles in base fluids e.g. water, and are responsive to the application of magnetic fields. To simulate the manufacture of such materials, magneto hydrodynamics provides an excellent platform. Furthermore many stable magnetic nanofluids are synthesized at high temperatures and this raises thermal radiative heat transfer (Zaid *et al*. [1]; Sergis *et al*. [2])
In this years a number of studies of magneto hydrodynamic nano fluid convection flows have been reported. These studies have stretched the inventive work into coolants of Choi at Argonne National Laboratory in the United States in the mid-1990s (Choi *et al*. [4]). the term nanofluid to describe fluids engineered by suspending small volumetric nanoparticles (*Cu*, *Al*, Al_2O_3, TiO_2, *SiC*, *SiN*, *AlN*) with normal sizes less than 100 nm in conventional heat transfer fluids (H_2O, $C_2H_6O_2$) and also other base fluids like engine oil, mineral oil, bio-fluids and poor heat transfer fluids. The thermal-enhancing properties of magnetic nanofluids have engrossed increasing interest in spreading fields such as electronics, optical devices, material synthesis, high power x-rays, lasers and biomedical sciences. Most studies of magnetic nanofluid transport have utilized the Lorentz magnetic body force formulation. (Oztop *et al*. [5]) studied the hydromagnetic natural convection in an enclosure from two semi-circular heaters on the bottom wall. (Chamkha and Aly [6]) reported on magnetic free convective flow of a nanofluid with heat sink/source effects. (Ellahi [7]) studied the MHD flow of non-Newtonian nanofluid in a pipe, the fourth order Runge-Kutta Shooting technique is engaged to investigate the unsteady MHD laminar convective nanofluid flow over permeable accelerated stretching vertical surface by Freidoonimehr *et al*. [8]. (Sheikholeslami *et al*. [9]) used a fourth-order Runge-Kutta method to study magneto hydrodynamic (MHD) nanofluid flow and heat transfer in a rotating parallel plate channel system, considering copper, silver, alumina and titanium oxide nano-particles suspended in water. They indicated that Nusselt number is a maximum for the titanium oxide-water nanofluid case whereas it is strongly reduced with increasing magnetic parameter.

(Ramzan and Bilal [10]) employed a homotopy method (HAM) to obtain power series solutions for three-dimensional flow of viscoelastic conducting nanofluid along a bidirectional stretching sheet with species diffusion and chemical reaction, showing that chemical reaction exerts a strong influence on temperature and nano-particle concentration transfer rate (Sherwood number). They also noted that temperature is elevated whereas nano-particle concentration reduced with increasing Brownian motion parameter whereas primary and secondary velocity are both suppressed with greater viscoelasticity of the nanofluid. Chemical reaction. Recently, Rashidi *et al*. [11] studied two dimensional laminar free convective boundary layer flow of an Ostwald-de Waele Power-law nanofluid induced by a steadily rotating infinite disk to a non-darcian fluid past an upward facing chemically reacting horizontal plate saturated in a porous medium by employing OHAM (Optimal Homotopy Analysis Method).

Thermal radiation is traditionally simulated in boundary layer flows with Rosseland's diffusion flux model, which approximates the radiative heat transfer as an algebraic flux model. Several investigators have addressed radiative effects on nanofluid transport. (Turkyilmazoglu and Pop [12]) derived analytical solutions using the Rosseland flux model for radiative heating effects on transient free convection nanofluid boundary layer flows, for copper, titanium, silver, aluminium oxide nanofluids. (Satya Narayana *et al*. [13]) derived perturbation solutions for radiative magnetic rotating nanofluid flow with heat generation in a porous medium, showing that greater radiative contribution significantly increases nanofluid temperatures. Very recently, (Siva Reddy and Thirupathi [14]) investigated heat and mass transfer effects on natural convection flow in the presence of volume fraction for copper-water nanofluid. (Uddin *et al*. [15]) investigated radiation flux and hydrodynamic, thermal and solutal slip effects on nanofluid extending/contracting sheet flow with lie group methods and shooting quadrature, noting that heat transfer rates are strongly influenced by radiative heat transfer as are nano-particle mass transfer rates. Further studies considering thermal radiation in nanofluid convection flows have been reported by (Ibanez *et al*. [16]) who considered entropy generation in MHD radiativenanofluid slip flow in micro-channels.

In the present article it is therefore consider transient magnetohydrodynamic (MHD) free convective boundary layer flow of nanofluids from a stationary vertical porous plate in porous media. Wall suction (lateral mass flux) and viscous heating effects are also incorporated. An attempt is made to investigate comprehensively, the influence of pertinent parameters on primary and secondary velocity distributions for the stationary plate ($\alpha = 0$) and moving cases as well as temperature and concentration distribution for three ways water base nanofluid:Cu-H_2O and Al_2O_3-H_2O and Tio2-H2O Generally two models are popular for simulating nanofluids, namely the (Buongiorno [17]) Buongiorno model (which includes many mechanisms but which emphasizes the contribution of Brownian diffusion and thermophoresisfor heat transfer enhancement) Very recently, Thirupati *et al*. [18] used finite The finite element method (FEM) computation is employed to study the dissipative double diffusive magneto-convective nanofluid from a rotating porous surface in porous midia The current study is relevant to high-temperature, magnetohydrodynamic (MHD) nanofluid materials processing systems employing in body forces.

2. Mathematical formulation of the problem

The schematic model of the coordinate system and the physical problem under investigation are depicted in Figure 1. The Cartesian coordinate system is selected such that the *x axis* is along the direction of the plate through which fluid flow in the upward direction is considered, *y axis* is perpendicular to the plate and *z axis* is normal to the *x y plane* i.e. transverse to the plane of the plate. Now consider the magnetohydrodynamic free convection flow with heat and mass transfer (species diffusion) of an electrically-conducting nanofluid from the semi-infinite vertical porous plate adjacent to a homogenous, isotropic porous medium, in the presence of uniform suction in a of reference. Darcy's model is employed for porous medium drag effects. The plate is assumed to be in rigid body with constant angular velocity, about the *y axis*. A uniform magnetic field of strength, B0, is imposed transversely to the flow i.e. along the *y-axis.*

2.1 Porous medium

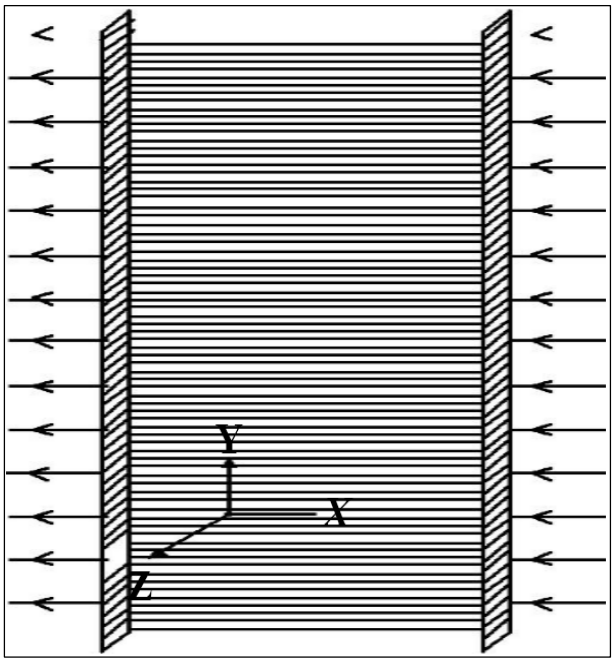

Fig 1

2.2 Physical model and coordinate system for the problem.

We considerthe three diamensionalunsteady, laminr natural convection flow electrically conducting nanofluid saturates porous medium is dissipative and is absorbing, emitting and gray but not scattering. Hall current and Maxwell displacement current effects are neglected *i.e. when t* 0along *x axis* direction against gravitational field, the temperature is raisedto T_w which is higher than the ambient temperature T and the species (nano-particle) concentration at the surface is maintained uniformly at C_w. Since the plate is assumed to be of infinite extent along *x and y* directions then all the physical quantities are dependent solely on *t and y*.

By considering the aforementioned assumptions the governing boundary layer equations of conservation of mass, momentum, energy and concentration equations by following Thirupati *et al*. [18] for magneto –convective nanoflluid are given by:

$$\frac{\partial w^*}{\partial y^*} = 0 \quad \text{….. (1)}$$

$$\rho_{nf}\left(\frac{\partial u^*}{\partial t^*} + w^*\frac{\partial u^*}{\partial y^*}\right) = \mu_{nf}\frac{\partial^2 u^*}{\partial y^{*2}} + g(\rho\beta)_{nf}(T^* - T_w^*) + g(\rho\beta)_{nf}(C^* - C_w^*) - -\sigma_{nf}B_0^2u^*\frac{v_f u^*}{k} \quad \text{..... (2)}$$

$$\rho_{nf}\left(\frac{\partial v^*}{\partial t^*} + w^*\frac{\partial v^*}{\partial y^*}\right) = \mu_{nf}\frac{\partial^2 v^*}{\partial y^{*2}} - \sigma_{nf}B_0^2 v - \frac{v_f v}{k} \quad \text{….. (3)}$$

$$(\rho\beta)_{nf}\left(\frac{\partial T^*}{\partial t^*} + w\frac{\partial T^*}{\partial z^*}\right) = k_{nf}\left(\frac{\partial^2 T^*}{\partial y^{*2}}\right) - \frac{\partial q_r}{\partial y^{*2}} + \mu_{nf}\left(\frac{\partial u^*}{\partial y^*}\right)^2 \quad \text{…. (4)}$$

$$\left(\frac{\partial c^*}{\partial t^*} + w\frac{\partial c^*}{\partial z^*}\right) = D_m\frac{\partial^2 c^*}{\partial y^{*2}} - k_r(C - C_\infty) \quad \text{…. (5)}$$

Where$(B)_{nf}$ are the volume of expansion, q_r is the radiative heat flux and D_m is the coefficient of chemical molecular diffusivity. Remaining symbols have the same meaning and corresponding initial and boundary conditions (Ishigaki [19]; Ganapathy [20]; Das *et al*. [21]) on the vertical surface and in the freestream can defined as:

$$for\ t \le 0\ \{\forall\ y$$

$$u(y,t) = 0, v = (y,t) = 0, T = T_\infty, C = C_\infty$$

$$for\ t > 0: y = 0$$

$$u(0,T) = \alpha u_0, v(0,t) = 0 \quad \text{… (6)}$$

$$T(0,t) = T_w + \epsilon(T_w - T_\infty)cosnt, C = C_w$$

$$for\ t > 0: y \to \infty$$

$$u(\infty,t) \to 0, v(\infty,t) \to 0, T(\infty,t) \to T_\infty, C(\infty,t) \to \infty$$

Here are velocity components along directions respectively and denotes the direction of motion of the plate. When the plate is said to be in stationary state and when this corresponds to the case where the plate is moving vertically upwards. It is worth mentioning here that nomenclature is presented in Appendix 1. The nanofluid properties (Oztop and Abu-Nada [22]) are given by:

$$\rho_{nf} = (1-\phi)_{\rho f} + \phi_s, \left(\rho c_p\right)_{nf} = (I-\phi)\left(\rho c_p\right)_f + \phi(\rho c_p)$$

$$\sigma_{nf} = \sigma_f\left[1 + \frac{3(\sigma-1)\phi}{(\sigma+2)(\sigma-1)\phi}\right], (\rho\beta)_{nf} = (1-\phi)(\rho\beta), \sigma = \frac{\sigma_s}{\sigma_f}\} \quad \text{… (7)}$$

The effective thermal conductivity of the nanofluid is adopted from brinkman [23] model as

$$\mu_{rf} = \frac{\mu_f}{(1-\phi)^{2.5}}$$

The effective thermal conductivity of the nanofluid is given by Maxwell – garnets model followed by Oztop and Abu-Nada [23]

$$k_{nf} = k_f\left[k_s + 2k_f - \frac{2\phi(k_f - k_s)}{k_s + 2k_f + 2\phi(k_f - k_s)}\right]$$

The continuity equation $\nabla.q = 0$ leads to the reduce mass conservation equation$\frac{\partial w}{\partial y} = 0$. On integrating the results $w = -w_0$ where constant w_0 is normal suction velocity at the plate and is constant. For an optically thick (photon mean free path is very

small) fluid, in addition to emission there is also self-absorption and usually the absorption coefficient is wavelength dependent so thus the net radiative heat flux term (Brewster [24]) is then approximated using the Rosseland diffusion model as:

$$q = -\frac{4\sigma^*}{3k}\frac{\partial T^4}{\partial y} \quad \ldots (8)$$

Here k^* andσ^* are the Rosseland mean absorption coefficient and Stefan-Boltzmann constant (5.6697*10-8Wm-2K-4) respectively. This model has been applied in a diverse range of both magnetic and non-magnetic heat and mass transfer problems and has been shown to be quite accurate for optically-dense regimes, as elaborated by (Beg *et al*. [25]). It is assumed that the temperature difference within the flow are sufficiently small such that may be expressed as a linear function of the temperature by expanding in a Taylor series about T_∞ as

$$T^4 \cong T_\infty^4 + 4T_\infty^3(T - T_\infty + 6T_\infty^2(T - T_\infty)^2 + \quad \ldots (9)$$

And by neglecting the higher order terms it gives

$$T^4 \cong 4T_\infty^3 T + 3T_\infty^4 \quad \ldots (10)$$

Proceeding with analysis for the non-dimensional variables defined as follows

$$y^* = \frac{u_0 y}{v_f}, u^* = \frac{u}{u_0}, t^* = \frac{u^2 t}{v_f}, n = \frac{vn}{u_0^2}, s = \frac{w_0}{u_0}, k = \frac{\rho_f k u_0^2}{v_f^2}, kr = \frac{k_r v_f}{u_0^2}, sc = \frac{v_f}{D_m}$$

$$\theta = \frac{T-T_\infty}{T_w-T_\infty}, C^* = \frac{c-c_\infty}{c_w-c_\infty}, M^2 = \frac{\sigma_f B_0^2 v_f}{\rho_f u_0}, R = \frac{16\sigma^* T_\infty^3}{3kk^*} \quad \ldots (11)$$

$$pr = \frac{(\rho c_p)_f v_f}{k_f}, E_c = \frac{u_0^2}{(\rho c_p)(T_w-T_\infty)}\ Gr = \frac{g\beta_f v_f (T_w-T_\infty)}{u_0^3}, Gc = \frac{g\beta_f v_f (c_w-c_\infty)}{u_0^3}$$

From the above equation that is equation (7)-(11) and substituting into equation (2)-(4) we obtain nanofluid properties and the above dimensionless variables we produce the following system of unsteady coupled, non-dimensional nonlinear partial differential equations.

$$\frac{\partial u}{\partial t} - S\frac{\partial u}{\partial y} = A_1\left(\frac{\partial^2 u}{\partial y^2}\right) - GrA_2C + GcA_2 - A_3\left(M^2 + \frac{1}{K}\right)u \quad \ldots (12)$$

$$\frac{\partial v}{\partial t} - S\frac{\partial v}{\partial y} = A_1\frac{\partial^2 v}{\partial y^2} - A_3\left(M^2 + \frac{1}{k}\right)v \quad \ldots (13)$$

$$\frac{\partial \theta}{\partial t} - S\frac{\partial \theta}{\partial y} = A_4\frac{\partial^2 \theta}{\partial y^2} + Ec\left(\frac{\partial u}{\partial y}\right)^2 \quad \ldots (14)$$

$$\frac{\partial c}{\partial t} - S\frac{\partial c}{\partial y} = \frac{1}{Sc}\frac{\partial^2 c}{\partial y^2} - Kr\ C + Sr\ \left(\frac{\partial^2 \theta}{\partial y^2}\right) \quad \ldots (15)$$

Where $A_1 = \frac{1}{(1-\phi)^{2.5}\rho_{nf}}, A_2 = \frac{(\rho c_p)_{nf}}{(\rho\beta)_{nf}}, A_3 = \frac{\sigma_{nf}}{\rho_{nf}}, A_4 = \frac{1}{(\rho c_p)_{nf} pr}\left(k_{nf} + R\right)$

In the above expression we consider the fraction volume of the nanofluid and the boundary condition of of the non diamensional equation form as:

$for\ t \leq 0\ \{\ \forall\ y$

$u(y,t) = 0, v = (y,t) = 0, T = T_\infty, C = C_\infty$

$for\ t > 0: y = 0$

$u(0,T) = \alpha u_0, v(0,t) = 0$

$T(0,t) = T_w + \epsilon(T_w - T_\infty)cosnt, C = C_w$

$for\ t > 0: y \to \infty$

$u(\infty,t) \to 0, v(\infty,t) \to 0, T(\infty,t) \to T_\infty, C(\infty,t) \to \infty \quad \ldots (16)$

The transformed system of non-linear, coupled of non-homogeneous dimensionless partial differential equations from equation (12)-(15) for the boundary conditions equation (16) are solved numerically by using the extensively-validated and robust finite element method with a Galerkin weighted residual scheme. This method comprises five fundamental steps, namely discretization of the domain, derivation of the element equations, assembly of element equations, imposition of boundary conditions description of these steps are presented in the (Thirupathy *et al*. [18]) and finally iterative solution of the assembled equations using matlab Details of the finite element approximations are provided below. Dimensionless primary velocity (u), secondary velocity (v), temperature (θ) and nano-particle concentration (C) are computed.
Formulation of variation with equation 12-15 over the two linear element $(y_\epsilon, y_{\varepsilon+1})$ is as follows:

$$\int_{y_\varepsilon}^{y_{\varepsilon+1}} w_1 \left[\frac{\partial u}{\partial t} - S\left(\frac{\partial u}{\partial y}\right) - A_1\left(\frac{\partial^2 u}{\partial y^2}\right) - GrA_2C + GcA_2 - A_3\left(M^2 + \frac{1}{K}\right)u\right] dy \quad \ldots (17)$$

$$\int_{y_\epsilon}^{y_{\epsilon+1}} w_2 \left[\frac{\partial v}{\partial t} - S\left(\frac{\partial v}{\partial y}\right) - A_1\left(\frac{\partial^2 v}{\partial y^2}\right) + A_3\left(M^2 + \frac{1}{k}\right)v\right] dy = 0 \quad \ldots (18)$$

$$\int_{y_\epsilon}^{y_{\epsilon+1}} w_3 \left[\frac{\partial \theta}{\partial t} - S\left(\frac{\partial \theta}{\partial y}\right) - A_4\left(\frac{\partial^2 \theta}{\partial y^2}\right)\right] dy = 0 \quad \ldots (19)$$

$$\int_{y_\epsilon}^{y_{\epsilon+1}} w_4 \left[\frac{\partial c}{\partial t} - S\left(\frac{\partial c}{\partial y}\right) - \frac{1}{Sc}\left(\frac{\partial^2 c}{\partial y^2}\right) + Kr\, C + Sr\left(\frac{\partial^2 \theta}{\partial y^2}\right)\right] dy = 0 \quad \ldots (20)$$

Where w_1, w_2, w_3, and w_4 are arbitrary observed functions and may be viewed as the variations in u, v, θ and C respectively. After reducing the order of integration and non-linearity, we arrive at the following system of equations.

$$\int_{y_\varepsilon}^{y_{\varepsilon+1}} \left[w_1\frac{\partial u}{\partial t} - Sw_1\left(\frac{\partial u}{\partial y}\right) - A_1\left(\frac{\partial w_1}{\partial y}\frac{\partial u}{\partial y}\right) - Grw_1A_2C - -Gcw_1A_2 + A_3w_1\left(M^2 + \frac{1}{K}\right)u\right] dy - \left[w_1\left(\frac{\partial v}{\partial y}\right)\right]_{y_\epsilon}^{y_{\epsilon+1}} = 0 \quad \ldots (21)$$

$$\int_{y_\epsilon}^{y_{\epsilon+1}} \left[w_2\frac{\partial v}{\partial t} - Sw_2\left(\frac{\partial v}{\partial y}\right) - A_1\left(\frac{\partial w_2}{\partial y}\frac{\partial v}{\partial y}\right) - A_3w_2\left(M^2 + \frac{1}{k}\right)v\right] dy - -\left[w_2\left(\frac{\partial v}{\partial y}\right)\right]_{y_\epsilon}^{y_{\epsilon+1}} = 0 \quad \ldots (22)$$

$$\int_{y_\epsilon}^{y_{\epsilon+1}} \left[w_3\frac{\partial \theta}{\partial t} - Sw_3\left(\frac{\partial \theta}{\partial y}\right) + A_4\left(\frac{\partial w_3}{\partial y}\frac{\partial \theta}{\partial y}\right)\right] dy - \left[w_3\left(\frac{\partial c}{\partial y}\right)\right] = 0 \ldots (23)$$

$$\int_{y_\epsilon}^{y_{\epsilon+1}} \left[w_4\frac{\partial c}{\partial t} - Sw_4\left(\frac{\partial c}{\partial y}\right) + \frac{1}{Sc}\left(\frac{\partial w_4}{\partial y}\right)\left(\frac{\partial c}{\partial y}\right) - Krw_4\, C + Sr\left(\frac{\partial^2 \theta}{\partial y^2}\right)\right] dy - \left[w_4\left(\frac{\partial c}{\partial y}\right) + Srw_4\frac{\partial \theta}{\partial y}\right]_{y_\epsilon}^{y_{\epsilon+1}} = 0 \quad \ldots (24)$$

The finite element model may be obtained from Equation. (17)-(20) By substituting finite element approximations of the form:

$$u = \sum_{i=1}^{2} u_j^\epsilon \psi_j^\epsilon,\ v = \sum_{i=1}^{2} v_j^\epsilon \psi_j^\epsilon,\ \theta = \sum_{i=1}^{2} \theta_j^\epsilon \psi_j^\epsilon,\ and\ C = \sum_{i=1}^{2} C_j^\epsilon\, \psi_j^\epsilon, \quad \ldots (25)$$

With $w_1 = w_2 = w_3 = w_4 (i = 1,2)\ where\ u_j^e, v_j^e, \theta_j^e$ and C_j^e are the velocities the direction of x- axis and y- axis respectively and temperature at the j^{th} node of $(y_\epsilon, y_{\epsilon+1})$ and ψ_j^ϵ are the function of this element $(y_\epsilon, y_{\epsilon+1})\ and\ taken\ as$:

$$\psi_1^\epsilon = \frac{y_{\epsilon+1} - y}{y_{\epsilon+1} - y_\epsilon} \text{And} \psi_1^\epsilon = \frac{y - y_\epsilon}{y_{\epsilon+1} - y_\epsilon}\ y_\epsilon \le y \le y_{\epsilon+1} \quad \ldots (26)$$

The finite element model of the equation for $\epsilon^{th} that\ form\ are\ as\ follows$:

$$\left[\begin{bmatrix} k_{11} & k_{12} & k_{13} & k_{14} \\ k_{21} & k_{22} & k_{23} & k_{24} \\ k_{31} & k_{32} & k_{33} & k_{34} \\ k_{41} & k_{42} & k_{43} & k_{44} \end{bmatrix}\begin{bmatrix} u^\epsilon \\ v^\epsilon \\ \theta^\epsilon \\ c^\epsilon \end{bmatrix}\right] + \left[\begin{bmatrix} M_{11} & M_{12} & M_{13} & M_{14} \\ M_{21} & M_{22} & M_{23} & M_{24} \\ M_{31} & M_{32} & M_{33} & M_{34} \\ M_{41} & M_{42} & M_{43} & M_{44} \end{bmatrix}\begin{bmatrix} u^{*\epsilon} \\ v^{*\epsilon} \\ \theta^{*\epsilon} \\ c^{*\epsilon} \end{bmatrix}\right] = \begin{bmatrix} b^{1\epsilon} \\ b^{2\epsilon} \\ b^{3\epsilon} \\ b^{4\epsilon} \end{bmatrix} \quad \ldots (27)$$

Where $\{[K_{mn}], [M_{mn}]\}\ and\ \{\{u^\epsilon\}, \{v^\epsilon\}\{\theta^\epsilon\}, \{c^\epsilon\}, \{u^{*\varepsilon}\}, \{v^{*\epsilon}\}, \{\theta^*\}, \{c^{*\epsilon}\}\ and\ \{b^{mn}\}\}$

$(m, n = 1,2,3,4)$Are the matrices of order 2x2 and 2x1 respectively and prime (*) indicates $\frac{\partial}{\partial y}$. $these$ matrice are define as follow:

$$K_{11}^{ij} = -S\int_{y_\epsilon}^{y_{\epsilon+1}} \left[\left[(\psi_i^\epsilon)\left(\frac{\partial \psi_j^\epsilon}{\partial y}\right)\right] dy + A_1\int_{y_\epsilon}^{y_{\epsilon+1}} \left[\left(\frac{\partial \psi_i^\epsilon}{\partial y}\right)\left(\frac{\partial \psi_j^\epsilon}{\partial y}\right)\right] dy\right] + A_3\left(M^2 + \frac{1}{k}\right)\int_{y_\epsilon}^{y_{\epsilon+1}} \left[(\psi_i^\epsilon)(\psi_j^\epsilon)\right] dy$$

$$K_{12}^{ij} = -2k^2\int_{y_\epsilon}^{y_{\epsilon+1}} (\psi_i^\epsilon)(\psi_j^\epsilon) dy\ K_{13}^{ij} = -GrA_2\int_{y_\epsilon}^{y_\epsilon+1} \left[(\psi_i^\epsilon)(\psi_j^\epsilon)\right] dy$$

$$M_{14}^{ij} = -GcA_2 \int_{y_\epsilon}^{y_\epsilon+1} \left[(\psi_i^\epsilon)(\psi_j^\epsilon)\right]dy M_{12}^{ij} = M_{13}^{ij} = M_{14}^{ij} = 0 \quad \ldots (28)$$

$$K_{22}^{ij} = -S \int_{y_\epsilon}^{y_{\epsilon+1}} \left[\left[(\psi_i^\epsilon)\left(\frac{\partial \psi_j^\epsilon}{\partial y}\right)\right]dy + A_1 \int_{y_\epsilon}^{y_{\epsilon+1}} \left[\left(\frac{\partial \psi_i^\epsilon}{\partial y}\right)\left(\frac{\partial \psi_j^\epsilon}{\partial y}\right)\right]dy\right] + A_3\left(M^2 + \frac{1}{k}\right)\int_{y_\epsilon}^{y_\epsilon+1} \left[(\psi_i^\epsilon)(\psi_j^\epsilon)\right]dy$$

$$K_{21}^{ij} = -2k^2 \int_{y_\epsilon}^{y_\epsilon+1} \left[(\psi_i^\epsilon)(\psi_j^\epsilon)\right]dy, K_{23}^{ij} = 0, K_{24}^{ij} = 0,$$

$$M_{22}^{ij} = \int_{y_\epsilon}^{y_\epsilon+1} \left[(\psi_i^\epsilon)(\psi_j^\epsilon)\right]dy, M_{21}^{ij} = M_{23}^{ij} = 0 \quad \ldots (29)$$

$$K_{31}^{ij} = 0, K_{32}^{ij} = 0, K_{34}^{ij} = 0,$$

$$K_{33}^{ij} = -S \int_{y_\epsilon}^{y_{\epsilon+1}} \left[\left[(\psi_i^\epsilon)\left(\frac{\partial \psi_j^\epsilon}{\partial y}\right)\right]dy + A_4 \int_{y_\epsilon}^{y_{\epsilon+1}} \left[\left(\frac{\partial \psi_i^\epsilon}{\partial y}\right)\left(\frac{\partial \psi_j^\epsilon}{\partial y}\right)\right]\right]dy$$

$$M_{31}^{ij} = 0, M_{32}^{ij} = 0, M_{33}^{ij} = \int_{y_\epsilon}^{y_\epsilon+1} \left[(\psi_i^\epsilon)(\psi_j^\epsilon)\right]dy, M_{34}^{ij} = 0 \quad \ldots (30)$$

$$K_{41}^{ij} = 0, K_{42}^{ij} = 0, K_{43}^{ij} = -Sr \int_{y_\epsilon}^{y_{\epsilon+1}} (\psi_i^\epsilon)\left[\left(\frac{\partial \psi_i^\epsilon}{\partial y}\right)\left(\frac{\partial \psi_j^\epsilon}{\partial y}\right)\right] dy$$

$$K_{44}^{ij} = -S \int_{y_\epsilon}^{y_{\epsilon+1}} \left[\left[(\psi_i^\epsilon)\left(\frac{\partial \psi_j^\epsilon}{\partial y}\right)\right]dy + \frac{1}{sc}\int_{y_\epsilon}^{y_{\epsilon+1}} \left[\left(\frac{\partial \psi_i^\epsilon}{\partial y}\right)\left(\frac{\partial \psi_j^\epsilon}{\partial y}\right)\right]dy\right] + Kr \int_{y_\epsilon}^{y_\epsilon+1} \left[(\psi_i^\epsilon)(\psi_j^\epsilon)\right]dy$$

$$M_{41}^{ij} = 0, M_{42}^{ij} = 0, M_{44}^{ij} = \int_{y_\epsilon}^{y_\epsilon+1} \left[(\psi_i^\epsilon)(\psi_j^\epsilon)\right]dy, M_{43}^{ij} = 0 \quad \ldots (31)$$

$$b_{1\epsilon}^i = \left[(\psi_i^\epsilon)\left(\frac{\partial u}{\partial y}\right)\right]_{y\epsilon}^{y\epsilon+1}, b_{2\epsilon}^i = \left[(\psi_i^\epsilon)\left(\frac{\partial u}{\partial y}\right)\right]_{y\epsilon}^{y\epsilon+1}$$

$$b_{3\epsilon}^i = \left[(\psi_i^\epsilon)\left(\frac{\partial \theta}{\partial y}\right)\right]_{y\epsilon}^{y\epsilon+1}, b_{4\epsilon}^i = \left[(\psi_i^\epsilon)\left(\frac{\partial C}{\partial y}\right) + Sr\left(\frac{\partial \theta}{\partial y}\right)\right]_{y\epsilon}^{y\epsilon+1} \quad \ldots (32)$$

3. Discussion

From fig: 2-4 shows the velocity, temperature, concentration, skin friction and the rate of heat transfer. Effects for different values of permeability parameter (K), velocity slip parameter (h1) on plate y = 0, the cross flow Reynold's number (Re), radiation parameter (R), the thermal Grashof number (Gr), mass Grashof number (Gc), Prandtl number (Pr), Schmidt number (Sc), z and λ are shown graphically. We specially observe the case of free flow (K = ∞) along with no slip for water (Pr = 7, Sc = 0.61) and for air (Pr=0.71, Sc=0.22). We fix Ec = 0.01, ∈ = 0.05 throughout our calculations, numerical computations have been performed. Here this article address the influence of $K^2, M^2, Sr, Gr, Gc, E, \phi, R, Pr, Sc, and\ kr$, on the nanofluid velocity, temperature and species concentration distributions. Solutions are showed the Numerical solutions are illustrated in these figures by fixing the values $n = 10, nt = \frac{\pi}{2}, \epsilon = 0.02\ t = 0.19\ and\ 0.5\ the$ n =10, NT =1/2, which is computed by using the mathematica for computation of velocity, temperature and concentration profiles. The following default values were adopted to represent physically realistic flows for finite element by (Thirupati *et al*. [18]

Graphically for briefness and are noted in other studies of nanofluid boundary layers. A parametric investigation is now undertaken to elucidate the thermo-physical characteristics of the flow. In all plots the asymptotic profiles for large y confirm that an adequately large boundary condition is imposed in the freestream and that solutions are indeed correctly converged. Depict the primary (*u*) and secondary (*v*) velocity (for 0 *and* 1 cases), temperature and concentration profile distributions for three different water-based nanofluids*Cu H* $_2O$ (copper water), Al_2O_3 *H* $_2O$ (Aluminium oxide-water) and TiO_2 *H* $_2O$ (Titaniumoxide-water).

4. Conclusions

A mathematical ideal has been presented for the passing incompressible MHD free convective boundary layer flow of nanofluids from a vertical porous plate considering, thermal radiation, viscous heating and chemical reaction effects. The non-dimensionalized partial differential equations for primary and secondary momentum, energy and species conservation which govern the flow problem have been solved numerically by using robust finite element method. Validation of solutions with earlier published results has been included. Mesh-independence study has also been conducted. Both cases of an upwardly moving plate and a stationary plate have been considered. Results have been computed and depicted graphically for influence of

k^2, M^2, *Sr*, *Gr*, *Gc*, *Ec*, *R*, Pr, *Sc* and *Kr* on the nanofluid velocity, temperature and species concentration distributions. Furthermore a variety of water based nanofluids i.e. *Cu* H_2O, $Al_2O_3H_2O$ and TiO_2H_2Onanofluids have been considered. The

numerical solutions have been presented at a selected time interval. The principal findings of the current investigation are summarized below.

The primary and secondary flow are both accelerated with increasing values of *Sr*, *Gr and Gc*, while they are decelerated with increasing values of k^2, M^2 *and* forboth stationary and moving plate cases. *Cu* H_2Onanofluid velocity distributions attains zero velocity asymptotically faster than the $Al_2O_3H_2O$nanofluid.An increase in *R* and *Ec*tends to elevate temperatures and therefore increases thickness of the thermal boundary layer. Conversely an increase in the parameters Pr decreases temperatures and reduce the thickness of thermal boundary layer. The nano-particle concentration magnitudes and therefore species concentration boundary layer increases with an increase of *Sr*, while increasing parameters *Scand Kr* manifests in a reduction in nano-particle concentrations and concentration boundary layer thickness. Greater thickness of thermal and concentration boundary layers is achieved for *Cu* H_2Onanofluid relative to $Al_2O_3H_2O$nanofluid. Soret number exert, via the thermal-diffusion and diffusion-thermo cross-flow gradient effects, a significant influence on heat and mass transfer characteristics of water based nanofluids.

Table 1: Thermo-physical properties of water and nanoparticles

Physical properties	*H2O*	*Cu*	*Ag*	*Al2O3*	*TiO2*
Cp(j/kg k)	4179	385	235	765	686.2
ρ(kg/m3)	997.1	8933	10500	3970	4250
K(W/m k)	0.613	401	429	40	8.9538
β X10^{-5}(1/k)	21	1.67	1.89	0.85	0.9
σ (S/m)	$5.5x10^{-6}$	$59.6x10^{6}$	$62.1x10^{6}$	$35x10^{6}$	$2.6x10^{6}$

Table 2: Comparison of Skin friction and Nusselt number for various values of *Pr* (*R* 0, *K*, *Ec* 0, *Gc* 0, *Sr* 0)

Pr	Previous results [18]		Present results	
	^{C}f	*Nu*	^{C}f	*Nu*
0.5	2.30	5.967	2.3200	5.9671
1.0	2.28	6.046	2.2581	6.0462
1.5	2.16	6.125	2.1961	6.1253S
2.0	2.14	6.206	2.1342	6.2060

Table 3: Comparison of Skin friction and Nusselt number for various values of *Pr* (*Gc* 0, *Ec* 0, *Sr* 0)

Pr	Previous results [37]		Present results	
	C_f	*Nu*	C_f	*Nu*
0.5	2.3159708	5.9674	2.3159801	5.9674102
1.0	2.2567503	6.0461	2.2567602	6.0461114
1.5	2.1972895	6.1259	2.1972743	6.1259021
2.0	2.1376083	6.2066	2.1376135	6.2066035

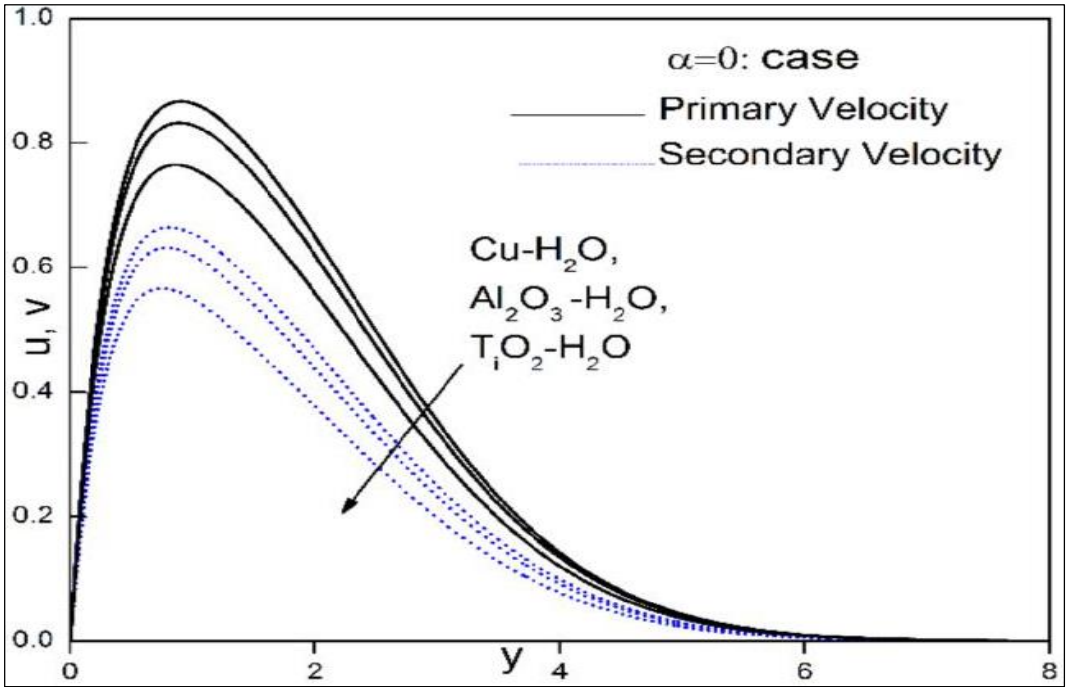

Fig 2: Velocity profiles for different nanofluids.

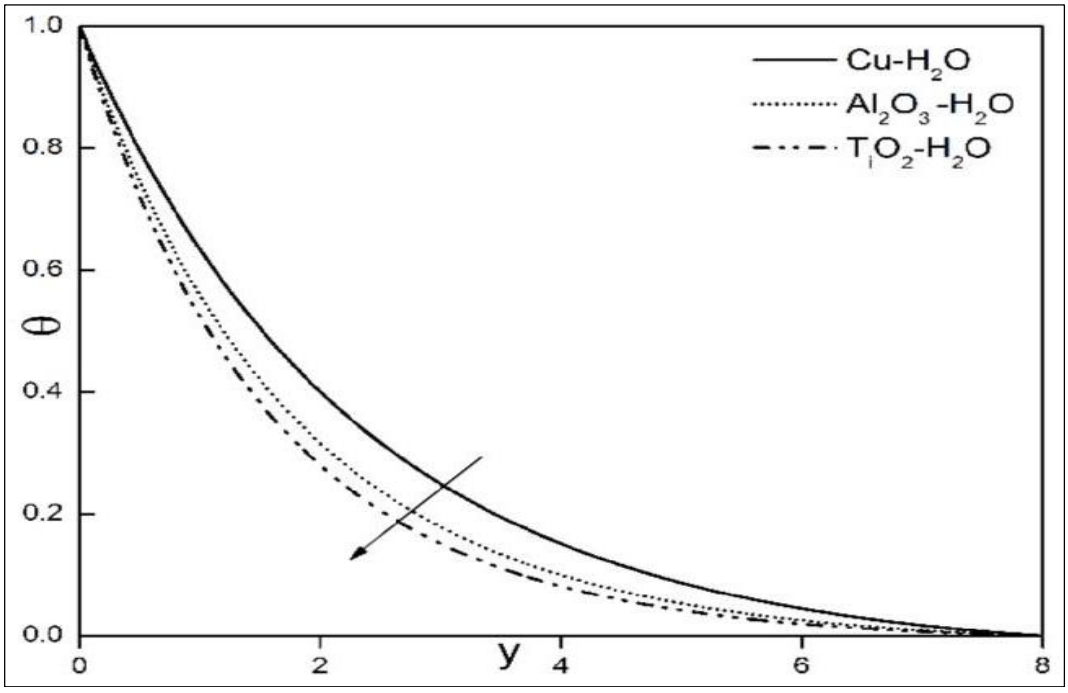

Fig 3: Temperature profiles for different nanofluids

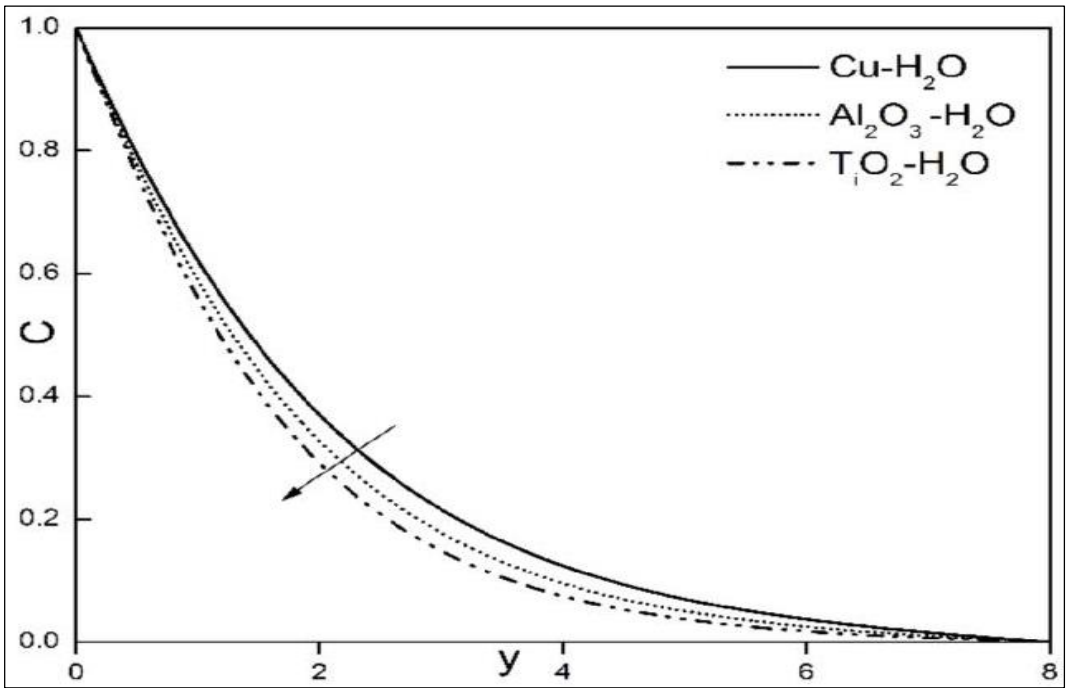

Fig 4: Concentration profiles for differentnanofluids

5. References

1. Zaid Z, Sajid MH, Saidur R, Kamalisarvestani M, Rahim NA. Radiative properties of nanofluids. Int. Comm. Heat Mass Transfer. 2013; 46:74-84.
2. Sergis A, Barrett T, ardalupas Y. Potential for improvement in high heat flux hyper vapotron element performance using nanofluids. Proc. 24th IAEA FEC, San Diego, USA, 2012.
3. Beg OA, Rashidi MM, Akbari M, Hosseini A. comparative numerical study of single-phase and two-phase models for Bio-nanofluid transport phenomena. Journal of Mech. In Medicine and Biology. 2014; 14(1):1450011.
4. Choi SUS, Zhang ZG, Yu W, Lockwood FE, Grulke EA. Anomalously thermal conductivity enhancement in nanotube suspensions. Appl. Phys. Lett. 2001; 79:2252.
5. Oztop HF, Rahman MM, Ahsan A, Hasanuzzaman M, Saidur R, Al-Salem KH *et al*. MHD natural convection in an enclosure from two semi-circular heaters on the bottom wall. Int. J Heat Mass Transfer. 2012; 55:1844-54.
6. Chamkha AJ, Aly AM. MHD free convection flow of a nanofluid past a vertical plate in the presence of heat generation or absorption effects. Chem. Eng. Comm. 2011; 198:425-441.
7. Ellahi R. The effects of MHD and temperature dependent viscosity on the flow of non-Newtonian nanofluid in a pipe: analytical solutions. Appl. Math. Model. 2013; 37(3):1451-67.

8. Freidoonimehr N, Rashidi MM, Shohel MD. Unsteady MHD free convective flow past a permeable stretching vertical surface in a nanofluid. Int. J Thermal Sci. 2015; 87:136-145.
9. Sheikholeslami M, Gorji-Bandpy M, Ganji DD, Rana P, Soleimani S. Magnetohydrodynamic free convection of Al2O3-water nanofluid considering thermophoresis and Brownian motion effects. Computers & Fluids. 2014; 94:147-160.
10. Ramzan Mand Bilal M. Three-dimensional flow of an elastico-viscous nanofluid withchemical reaction and magnetic field effects. J Molecular Liquids. 2006; 200: 212-220.
11. Rashidi MM, Momoniat E, Ferdows M, Basiri PA. Lie-group solution for free convective flow of nanofluid past a chemically reacting horizontal plate in a porous media. Mathematical Problems in Eng, 2014.
    Article ID: 239082.
12. Turkyilmazoglu Mand Pop I. Heat and mass transfer of unsteady natural convection flowof some nanofluids past a vertical infinite flat plate with radiation effect. Int. J Heat andMass Transfer. 2013; 59:167-171.
13. Satya Narayana PV, Venkateswarlu B, Venkataramana S. Thermal radiation and heat source effects on a MHD nanofluid past a vertical plate in a rotating system with porous medium. Heat Transf Asian Res. 2015; 44(1):1-19.
14. Siva Reddy S, Thirupathi T. Heat and Mass transfer effects on natural convection flow in the presence of volume fraction for copper-water nanofluid. J Nanofluids. 2016; 5:220-230.
15. Uddin MJ, Beg OA, Aziz A, Ismail AI Md. Group analysis of free convection flow of a magnetic nanofluid with chemical reaction. Mathematical Problems in Engineering, 2015.
    Article ID 621503, 11 pages http://dx.doi.org/ 10.1155/2015/621503.
16. Ibanez G, Lopez A, Pantoja J, Moreira J. Entropy generation analysis of a nanofluid flow in MHD porous microchannel with hydrodynamic slip and thermal radiation. Int. J.Heat and Mass Transfer. 2016; 100:89-97.
17. Buongiorno J. Convective transport in nanofluids. ASME J Heat Transfer. 2006; 128:240-250.
18. Thirupatithumma Anwar O, Reddy S. Sheri finite differentially heated square cavity utilizing nanofluids. Int. J Heat Mass Transfer. 2007; 50:2002-2018.
19. Ishigaki H. Periodic boundary layer near a two-dimensional stagnation point. J Fluid Mech. 1970; 43:477-486.
20. Ganapathy R. A note on oscillatory Couette flow in a rotating system. ASME J Appl. Mech. 1994; 61:208-209.
21. Das S, Jana RN, Chamkha AJ. Magnetohydrodynamic free convective boundary layer flow of nanofluids past porous plate in a rotating frame. J Nanofluids. 2015; 4:176-185.
22. Oztop HF, Abu-Nada E. Numerical study of natural convection in partially heated rectangular enclosures filled with nanofluids. Int. J Heat Mass Transfer. 2008; 29:1326-1336.
23. Brinkman HC. Viscosity of concentrated suspension and solution. J hem. Phys. 1952; 20:571-581.
24. Brewster MQ. Thermal radiative transfer properties. Wiley: New York, 1972.
25. Beg OA, Zueco J, Takhar HS, Beg TA, Sajid A. Transient non-linear optically-thick radiative-convective double-diffusive boundary layers in a darcian porous medium adjacent to an impulsively started surface: network simulation solutions. Comm. Nonlinear Science and Numerical Simulation. 2009; 14:3856-3866.
26. Beg OA, Zueco J, Ghosh SK, Heidari A. Unsteady magnetohydrodynamic heat transfer in a semi-infinite porous medium with thermal radiation flux: analytical and numerical study. Advances in Numerical Analysis.
    Article ID 304124, pp. 1-17, DOI: 10.1155/ 2011/ 304124.